



Development of an Innovative 3D-Printing Process for Reinforced Concrete – AMoRC Method

Sisi Zhang^(✉), Matthias Kalus, Sven Engel, Josef Hegger, and Martin Claßen

Institute of Structural Concrete, RWTH Aachen, Aachen, Germany
szhang@imb.rwth-aachen.de

Abstract. In this paper, a novel 3D printing process for reinforced concrete structures called Additive Manufacturing of Reinforced Concrete (AMoRC) is proposed. The process consists of a continuous concrete extrusion process and an intermittent stud welding process, both carried out by a robotic arm respectively. The welding robot runs ahead of the concrete extrusion robot and produces the spatial reinforcement mesh from prefabricated reinforcing bar segments. A novel fork-shaped print head with four adjustable nozzles allows for concrete extrusion around the reinforcement with different diameters. By joining segmented rebars of limited length to a reinforcement mesh in the AMoRC process, the consumption of energy and time can drastically be reduced compared to shape welding. The length of the joined rebars can be adapted to the component geometry and the extrusion speed. The bar segments to be joined are kept ready in a magazine belonging to the print head, which enables the feeding of bars with different diameters to arrange a load-efficient and economical reinforcement mesh. The preliminary testing of the additively fabricated reinforced concrete components is also implemented to characterize the structural behaviour of those 3D-printed composite specimens. In the initial phase, the reinforcement installation was performed manually until the second robot will be added to the process and experiments were done to characterize the printed structures. The pull-out test is used to investigate the bonding behavior between reinforcement and printed concrete. The four-point bending test is also utilized to study the mechanical behavior of the printed reinforced concrete specimen in a larger scale.

Keywords: 3D-printing of reinforced concrete · AMoRC method · characterisation methods · pull-out test · 4-point bending experiment

1 Introduction

3D Concrete Printing (3DCP) [1, 2] belongs to Additive Manufacturing (AM) technologies in the field of digital fabrication with concrete (DFC) [3], which has been entering gradually the construction sector since the mid-1990s aiming for more sustainable structures with higher productivity, e.g., less carbon footprint due to more load-efficient construction of members. In the beginning the AM process was used in the construction

sector to just print the outer contour of a component [1]. Afterwards, various processes were developed which enable the printing of entire structures by means of additive production [4, 5]. Since then, numerous universities and companies have started to develop 3D printing processes for concrete leading to a continuously growing research community. However, most of the printed concrete structures nowadays are unreinforced, which prevent the further development of 3DCP because the reinforcement is mandatory in most structural applications to satisfy key requirements such as loading-carrying capacity, ductility, robustness, etc. [6]. Until now, several attempts were tried to integrate the reinforcement in the printing process. Based on the sequence of adding reinforcement, it could be classified as (1) printing or placing reinforcement in advance in the formwork before casting, e.g., Digital Casting System in ETH Zurich [7], or Shotcrete 3D Printing in TU Braunschweig [8]; (2) adding reinforcement simultaneously to the concrete printing, e.g., integrating fibre or textile reinforcement in the concrete extrusion process, which allows for reinforcement parallel to the extrusion direction [9]; (3) adding reinforcement after the printing process, such as Contour Crafting method that firstly printing the external concrete contour as a lost formwork and then post-install the reinforcement in the contour which is subsequently filled with concrete [1]. A more detailed overview over the most important concepts for the integration of reinforcement and their review can be found in [10]. So far, a printing concept for reinforced concrete which does not require any manual work steps, fulfill all requirements for the properties of printed composite material and is applicable in the construction sector is still lacking.

2 Additive Manufacturing of Reinforced Concrete Process (AMoRC)

2.1 Development of the Process

In the following, the conceptual design of a novel 3D printing process for reinforced concrete, the so-called Additive Manufacturing of Reinforced Concrete (AMoRC), is presented. The proposed process is visualized in Fig. 1. The process uses two robotic arms, one for formwork-free depositing of concrete filaments and the other for installation of the reinforcement. The welding robot runs ahead of the concrete extrusion process and produces the spatial reinforcement mesh from prefabricated reinforcing bar segments. The concrete is placed around the reinforcing bars in such a way that they protrude a few centimeters from the printed concrete. The end zones of reinforcement bars sticking out of the concrete body can be used for attaching a next row of bar segments in subsequent layers of the printing process. In this way it is possible to create two- or three-dimensional reinforcement meshes bridging interfaces between subsequent layers of concrete and to simultaneously encase them with concrete. The result of combining the intermittent welding production process and the continuous concrete extrusion process is AMoRC, a hybrid production process for RC structures.

By joining segmented rebars of limited length to a reinforcement mesh in the AMoRC process, the consumption of energy and time can drastically be reduced compared to shape welding. The length of the joined rebars can be adapted to the component geometry and the extrusion speed. The bar segments to be joined are kept ready in a magazine

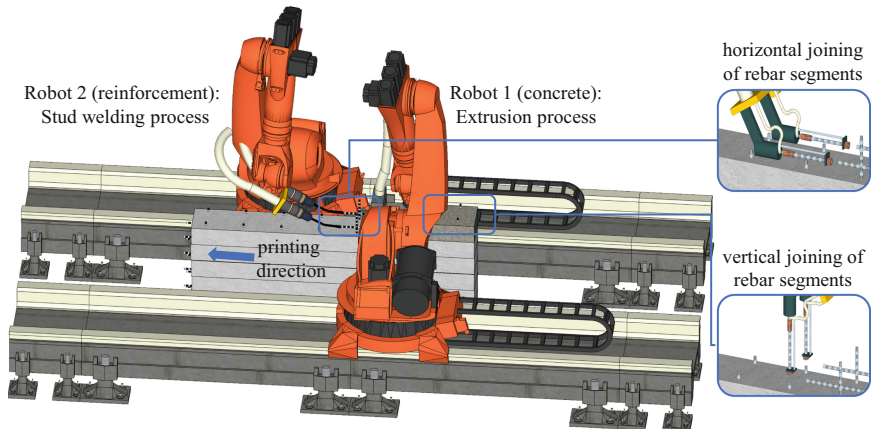


Fig. 1. 3D printing process (AMoRC) for production of reinforced concrete including concrete extrusion and stud-welding of reinforcement.

belonging to the print head, which enables the feeding of bars with different diameters. Due to the fact that the AMoRC process is not limited to a specific reinforcement diameter, the reinforcement mesh can be arranged load-efficient and thus economical. Furthermore, since the force transmission between the reinforcement segments is ensured by welding of the rebars, overlapping joints of the reinforcement can be avoided. Thus, less material is needed and possible weak points in the structure due to overlapping of the reinforcement can be excluded.

The concrete is deposited around the reinforcement by means of a concrete print head, which consists of fork-like arranged individual nozzles. Two nozzles are required for each layer of reinforcement to be encased with concrete. The distance between these nozzles can be adjusted to the current reinforcement diameter. The AMoRC process is particularly suitable to produce vertical free-standing, horizontally supported or slightly inclined structures. Details on the conception and development of the concrete print head, the nozzle arrangement, and their geometry as well as the general feasibility of the process are explained in [10]. In this paper, the focus lays on the preliminary testing results of the mechanical properties of the printed reinforced components based on an initial application of the AMoRC process.

2.2 Application of the Process

In the laboratory of the Institute of Structural Concrete at the RWTH Aachen, a printing setup consisting out of a 7-axes kinematic system visualized in Fig. 2 was established: A 6-axes KUKA robot KR 300 R2700–2 with a KRC4 control system installed on a KUKA linear unit KL 4000 1CA with a length of 5.5 m. For a constant material flow a m-tec duo mix concrete pump was added to the printing setup with a hose length of 15 m. At the end of the hose a customized extruder tool (nozzle) with a $45 \times 12 \text{ mm}^2$ opening is attached. A new welding unit was purchased for joining of the segmented rebars. However, the reinforcement installation is performed manually until the second robot will be added to

the process in the first half of 2023. To control all devices simultaneously – two robotic arms, concrete pump, and welding unit – a programmable logic controller (PLC) is used as a master control unit. In the present study however, the pump is manually controlled and thus, only the print path is programmed with the PLC. With this printing setup first component experiments described in the next chapter were conducted.

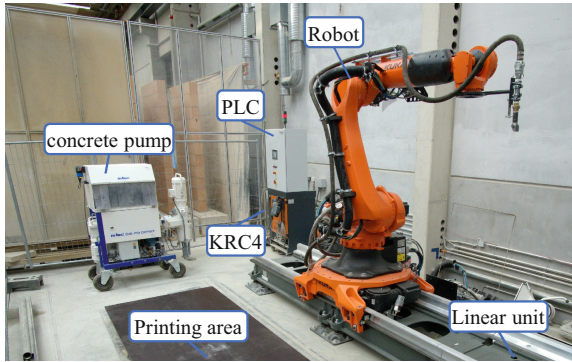


Fig. 2. 3D printing setup in laboratory.

Meanwhile, further investigations to complete and build up the AMoRC process are envisaged. To analyze the bond properties of encased rebars, pullout tests are planned for the longitudinal, horizontal, and vertical reinforcement directions. The load-capacity of printed reinforced concrete component will be studied by 4-point bending tests. Furthermore, systematic research into modified arc stud welding for joining reinforcement is planned, in which various possibilities for joining bars of different diameters at any desired angles in space will be explored. The quality of welded joints will be assessed by tensile, macrosection and hardness tests etc. Finally, the methods developed for concrete extrusion and rebar welding are combined into a simultaneously running hybrid process.

3 Experiment Investigation of the Printed Reinforced Concrete Components

3.1 Material

In the experiment, the *Weber 3D 145-2* with compressive strength class of C35/45 from *Saint-Gobain Weber* was used, which consists of Portland cement CEM I, limestone, fibres, admixtures, and aggregates with a maximum size of 1 mm. The dry materials were mixed continuously by the pump with a water flow rate of 240–250 l/h. The compressive strength (f_{cm}) and flexural strength ($f_{ctm,fl}$) of the mortar used in the experiments were determined on prisms with a dimension of 40x40x160 mm³ at the age of 28 days according to EN 196-1 [11].

Two kinds of reinforcement were used in the experiment. One is conventional ribbed steel bar B500 according to DIN 488 [12], which has a yield strength of 500 N/mm² and

a tensile strength of 550 N/mm^2 . Another reinforcing bar is welded threaded bolt, which is welded by several threaded bolts with length of 100 mm. The diameter of 10 mm was chosen for both kinds of reinforcing bars, see Fig. 3.

3.2 Experiment Programme

Pull-out Test. In the preliminary tests, the bonding between printed concrete and reinforcement was investigated by pull-out tests. Both conventional reinforcing rebars and welded treaded bolts with a diameter (d_s) of 10 mm in three orientations (i.e., parallel to the printing direction denoted as u -direction, perpendicular to printing direction in the print plane denoted as v -direction, and perpendicular to the print plane denoted as w -direction) are studied. The geometry of the specimen is a cube with a height of $10 \cdot d_s$ and bond length $l_b = 5 \cdot d_s$ according to RILEM Recommendation RC6 [13]. The reinforcement with a diameter of 10 mm with a length of 350 mm were used in the bonding experiments. The rebar has a length of 100 mm in the concrete body, which is divided into a 50 mm bonding area and a 50 mm non-bonding area isolated by a plastic sleeve. In addition, 200 mm of reinforcement bar length was required for later placement in the test setup in order to apply the tensile force at bar end. It was also planned to leave 50 mm of rebar sticking out on the other side of the concrete cube in order to measure the slip there using Linear variable displacement transducer (LVDT). What's more, the protrusion of the bar could also serve to fix itself in the formwork for the casted specimens.

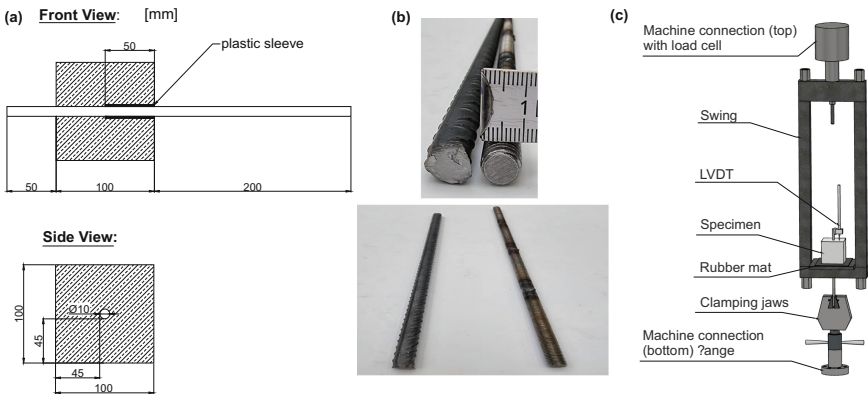








Fig. 3. Pull-out test: (a) geometry of the specimen; (b) reinforcement types; and (c) testing setup.

The pull-out test setup consists of a swing bolted to a 100 kN spindle testing machine Instron 5582. The specimen was clamped at its long reinforcement bar end by means of clamping jaws and rested on the supporting surface of the swing. A rubber mat between specimen and supporting surface ensured a better force transmission and less friction. There was a hole in the middle of the supporting surface of the swing and rubber mat, so that the rebar could be through it and be pulled out by the clamping jaws, which is attached to the machine connection on the bottom by means of a flange. Thus, the rebar was held at the bottom and the machine including the swing was controlled with a speed

of 1 mm/min during the tests. The slip of the rebar was recorded by a LVDT attached to the shorter rebar end of the specimen. The geometry, reinforcement types, and testing setup for the pull-out test is summarized and depicted in Fig. 3.

Besides the investigation of reinforcing types and reinforcement orientations, the influence of time interval on the bonding between conventional reinforcement and printed concrete was also studied. Furthermore, casted specimens with conventional reinforcement were also produced as references. A summary of the whole experience programme is listed in Table 1.

Table 1. Overview of the experiment program for pull-out test.

Descriptions	Sketch	Reinforcement type	Number of specimens
Casted specimen		Conventional	3
Printed specimen with reinforcement in <i>u</i> -direction		Conventional	3
		Welded	3
Printed specimen with reinforcement in <i>v</i> -direction		Conventional	3
		Welded	3
Printed specimen with reinforcement in <i>w</i> -direction		Conventional	3
		Welded	3
Printed specimen with reinforcement in <i>u</i> -direction with time interval of 1h		Conventional	3
Printed specimen with reinforcement in <i>u</i> -direction with time interval of 12h		Conventional	3

4-Point Bending Test. In order to estimate the printed reinforced component in large-scale, four-point bending tests on reinforced concrete beams with a length of 1600 mm, width (b) of 100 mm and height (h) of 160 mm, which are reinforced with two normal strength steel bars (B500) with a diameter of 10 mm, were conducted. The effective depth (d) of the reinforced beam is 130 mm. In the preliminary tests, two casted and one printed reinforced beams were tested, see Fig. 4. For the printed specimen, each layer of the beam consists of two filaments printed side by side with a layer height of approximately 11 mm and a printing speed of 210 mm/s. Even if the parameters in the pump are set constant, the material consistency and thus the filament width can differ. The width of the cross-section of the printed specimen deviated between 140 mm at the bottom and 120 mm at the top. The reinforcement was placed manually between the second and the third layer with a concrete cover of 25 mm. After printing, the component was cut on both ends to achieve the beam length of 1600 mm with flat surfaces. Furthermore, a smooth surface for the loading was created with gypsum.

The beams were supported on two roller bearings in a distance of 1500 mm. The deflections of the specimens were measured with two LVDTs at two sides of the mid-span. The testing loads were applied by machine Instron 5582 on two points in 150 mm at mid-span with a displacement rate of 0.5 mm/min.

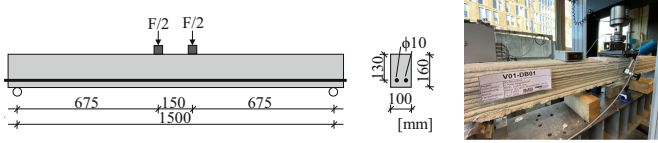


Fig. 4. Test setup, geometry, and reinforcement of the specimens.

3.3 Experiment Results

Material Test. In order to convert the measured compressive strengths of the half-prisms to the compressive strength of the standard test specimens (i.e., cube with 150 mm edge length and cylinder with diameter of 150 mm and height of 300 mm) for classification of concrete compressive strength classes, the following conversions based on Eq. (1) and Eq. (2) must be made:

$$f_{ck,cyl} = (f_{c,pr} \cdot 0.9 - 8) \cdot 0.92 \quad (1)$$

$$f_{ck,cube} = (f_{c,pr} \cdot 1.06 - 8) \cdot 0.92 \quad (2)$$

where the $f_{ck,cyl}$ and $f_{ck,cube}$ are the characteristic values of concrete compressive strength of cylinder specimen and cube specimen respectively; and $f_{c,pr}$ is the mean value of tested compressive strength of the half-prisms. The factor 0.9 and 1.06 come from own experiment results in the institute [14] for transformation of compression strength from prisms to cylinders or cubes. The value 8 is the difference between characteristic and mean values, while the factor 0.92 is a calibration value for concrete curing in air instead of in water based on DIN 1045-2 [15].

The specimens were made in several different printing days and the water flow vary from 240–250 l/h. The measured flexural and compressive strengths for each specimen are summarized in Table 2 and Table 3.

Pull-out Test. The existing bonding stress τ that occurs during tests could be calculated using the applied force F relative to the bonding area $A_b = U_b \cdot l_b$ in Eq. (3) [13]:

$$\tau = \frac{F}{U_b \cdot l_b} \cdot \frac{f_{cm}}{f_c} = \frac{F}{5 \cdot \pi \cdot d_s^2} \cdot \frac{f_{cm}}{f_c} \quad (3)$$

where f_{cm} is the mean value of concrete compressive strength class (here = 43 N/mm²), and f_c refers to the mean value of tested specimens. The factor $\frac{f_{cm}}{f_c}$ could also be transferred

to the ratio of characteristic values $\frac{f_{ck}}{f_c}$, where f_c here denotes characteristic value of tested results and could be calculated by Eq. (1) or Eq. (2).

There are different types of failure when the pull-out tests were implemented: (a) splitting failure (SP), where crack propagates in the surrounding concrete due to the bar’s wedging action; (b) welding joint failure (WJ), where the welded joints break during the tests; and (c) slipping failure (SL) due to the debonding of the reinforcement and surrounding concrete. The former two failure types are brittle fracture, while the last slipping failure is ductile failure, see Fig. 5. For pull-out tests, the slipping failure is preferred to study the bond between reinforcement and concrete.

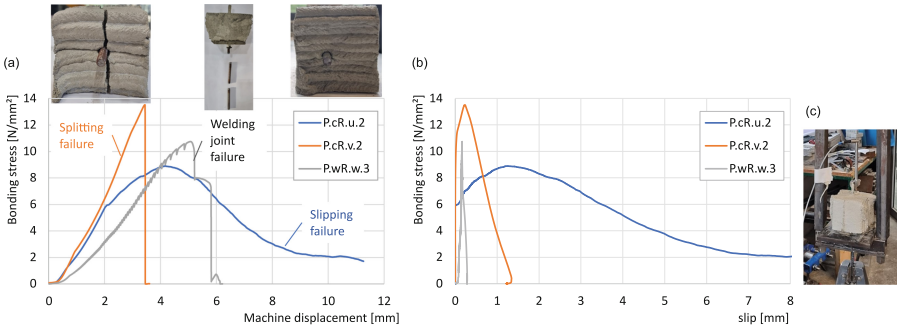


Fig. 5. Results of pull-out test: (a) bonding stress-machine displacement relationship; (b) bonding stress-slip relationship; (c) testing setup

An overview of the testing results including failure type, maximum force (F_{max}), maximum bonding stress (τ_{max}), slip at maximum bonding stress (S_0), and concrete compression strength ($f_{ck,cyl}$) are listed in Table 2. The labelling of the specimens characterizes the main parameters of the experiments. The first letter *P* and *C* denotes printed and casted specimens respectively. The reinforcement types are specified by *cR* for conventional reinforcement and *wR* for welded reinforcement. The reinforcement orientations (*u*, *v*, and *w*) and specimen numberings (*1*, *2* and *3*) are also included in the labelling.

It could be found that the concrete geometry based on casting method cannot guarantee a slipping failure of printed specimens. In the preliminary tests, splitting failure is dominated, which leads to an underestimation of the bonding stress. To improve the results and to avoid splitting failure, the specimen geometry should be modified. The printed specimen with small size could then be confined with casted concrete to larger geometry ($200 \times 200 \times 200 \text{ mm}^3$). What’s more, it could also be found that the welded joints are weak points of the reinforcement, which also leads to underestimation of the bonding stress. In the further study, tensile tests of the welded reinforcement should be implemented. The welding joints should only be embedded in the bonding length area and the rest of the reinforcement should be continuous. In this case, the influence of welding joints on the bonding behavior could be studied without fracture of the welding joints outside bonding area.

It could be seen from the above Table 2, the printed and casted specimens have generally similar bonding strength. The reinforcement orientation in *w*-direction has the

Table 2. Overview of the measurement results of pull-out test.

Specimen name	Failure type	F_{max} [kN]	τ_{max} [N/mm ²]	Mean value of τ_{max} in one series [N/mm ²]	S_0 [mm]	$f_{ck, cyl}$ [N/mm ²]
C.cR.1	SP	18.81	10.18	9.28	1.14	41.08
C.cR.2	SP	16.39	8.87		0.95	41.08
C.cR.3	SP	16.23	8.78		0.46	41.08
P.cR.u.1	SL	14.13	9.00	10.53	1.31	35.4
P.cR.u.2	SL	13.98	8.90		1.26	35.4
P.cR.u.3	SP	25.30	13.69		0.21	41.08
P.cR.v.1	SP	13.98	7.56	8.76	0.16	41.08
P.cR.v.2	SP	21.23	13.52		0.22	35.4
P.cR.v.3	SL	8.15	5.19		1.04	35.4
P.cR.w.1	SP	26.97	14.59	12.90	0.76	41.08
P.cR.w.2	SP	20.99	11.36		0.22	41.08
P.cR.w.3	SP	23.55	12.74		0.12	41.08
P.cR.u.1h.1	SP	10.71	5.80	5.74	0.18	41.08
P.cR.u.1h.2	SP	10.62	5.75		0.18	41.08
P.cR.u.1h.3	SP	10.49	5.68		0.04	41.08
P.cR.u.1h45.1	SP	7.91	4.28	4.01	0.03	41.08
P.cR.u.1h45.2	SP	6.88	3.72		0.32	41.08
P.cR.u.1h45.3	SP	7.43	4.02		0.38	41.08
P.wR.u.1	SL	7.54	4.08	8.04	0.25	41.08
P.wR.u.2	SP	21.53	11.65		0.40	41.08
P.wR.u.3	SL	15.49	8.38		0.31	41.08
P.wR.v.1	SP	22.69	12.28	11.95	0.04	41.08
P.wR.v.2	WJ	22.62	12.24		0.66	41.08
P.wR.v.3	SP	20.96	11.34		0.09	41.08
P.wR.w.1	WJ	24.57	13.30	12.07	0.19	41.08
P.wR.w.2	WJ	22.49	12.17		0.53	41.08
P.wR.w.3	WJ	19.86	10.75		0.16	41.08

largest bonding stress in this experiment with both conventional and welded reinforcement. However, conventional- and welded reinforcement showed different behaviors in u- and v-directions. Nevertheless, the results in these series have large scatter, which

requires furthermore researches to obtain a plausible conclusion. What’s more, the time interval longer than 1h leads to dramatic decrease of bonding stress.

4-Point Bending Test. In the Table 3, the testing results as well as the beam geometry, concrete compressive strength $f_{ck,cyl}$ and flexural strength $f_{ctm,fl}$ are summarized. To account for deviations in the cross section dimensions the occurring shear force is normalized by the width and the effective depth of the respective beam.

Table 3. Overview of the measurement results of 4-point bending test.

Specimen name	F_{max} [kN]	V_{max} [kN]	V_{max}/bd [kN]	h [mm]	b [mm]	Water [l/h]	$f_{ck,cyl}$ [MPa]	$f_{ctm,fl}$ [MPa]
V01-DB01	32.4	16.2	1.04	150–160	120–140	250	45.96	7.5
V01-GB01	30.1	15.1	1.16	160	100	250	45.96	7.5
V01-GB02	34.4	17.2	1.32	160	100	240	48.78	7.8

The normalized load stress-deflection relationship and the crack patterns of tested beams are depicted in Fig. 6. In all beams bending cracks in the middle of the span were visible. In both conventional casted beams, a brittle shear failure occurred due to the absence of shear reinforcement. The load-deformation behavior of the printed beam, however, depicted a pronounced horizontal plateau where the reinforcement started to yield. The ratio between the normalized load bearing capacity of the printed and the conventional manufactured specimen was $1.04/1.16 = 0.90$. The specimen with a stiffer concrete consistency (water content 240 l/h instead of 250 l/h) could carry a higher ultimate load.

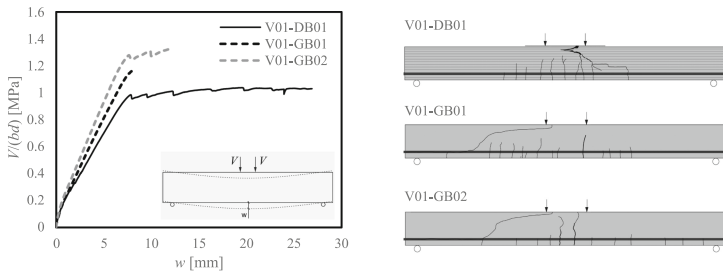


Fig. 6. Normalized load stress – deflection relationship of tested beams and their crack patterns

For general statements regarding the load bearing capacity of printed components more systematic test campaigns are needed. However, this first small test series indicates that the load bearing capacity of additive manufactured components is close to capacity of conventional manufactured components. The two casted beams showed critical shear cracks at failure leading to brittle failure due to the lack of shear reinforcement, while the printed beam was dominated by bending cracks causing a ductile failure since the tensile

reinforcement were integrated. For next tests, parameters such as specimen dimensions and the amount of reinforcement will be adjusted to get the same failure for all specimens.

4 Conclusion and Outlook

In this paper, the development and execution of a novel AM process for production of reinforced concrete was presented. In the hybrid AMoRC process, segmented steel reinforcing bars are joined to form a three-dimensional reinforcement mesh using a stud welding process and a concrete extrusion process simultaneously. The concept, in which general feasibility was proven with prototypical studies, was developed aiming for a more sustainable construction process matching with the requirements of construction sites and prefabrication plants. The decisive advantage of the developed method compared to previous approaches for 3D printing of reinforced concrete is the possibility to adjust the welding process and the concrete extrusion process for operation at identical feed rates. Synchronization of both processes allows combining them in one hybrid print head for production of reinforced concrete.

Preliminary experiments indicate that the load bearing capacity of additive manufactured components is close to the capacity of conventional manufactured using the material in this experiment programme. To ensure a satisfactory structural performance of the composite material, further research is needed to systematically study the bond behavior between reinforcement and concrete using self-developed fork-shaped nozzle with modified specimen geometry, where slipping failure dominates. What's more, shear reinforcement will also be integrated in the printed beams to study the shear behavior of printed beams.

References

1. Khoshnevis, B.: Automated construction by contour crafting—related robotics and information technologies. *Autom. Constr.* **13**(1), 5–19 (2004). <https://doi.org/10.1016/j.autcon.2003.08.012>
2. Paul, S.C., van Zijl, G.P., Tan, M.J., Gibson, I.: A review of 3D concrete printing systems and materials properties: Current status and future research prospects. *Rapid Prototyp. J.* **24**(4), 784–798 (2018). <https://doi.org/10.1108/RPJ-09-2016-0154>
3. Gebhard, L., Esposito, L., Menna, C., Mata-Falcón, J.: Inter-laboratory study on the influence of 3D concrete printing set-ups on the bond behaviour of various reinforcements. *Cement Concr. Compos.* **133**, 104660 (2022). <https://doi.org/10.1016/j.cemconcomp.2022.104660>
4. Lim, S., Buswell, R.A., Le, T.T., Austin, S.A., Gibb, A., Thorpe, T.: Developments in construction-scale additive manufacturing processes. *Autom. Constr.* **21**, 262–268 (2012). <https://doi.org/10.1016/j.autcon.2011.06.010>
5. Buswell, R.A., Leal de Silva, W.R., Jones, S.Z., Dirrenberger, J.: 3D printing using concrete extrusion: A roadmap for research. *Cem. Concr. Res.* **112**, 37–49 (2018). <https://doi.org/10.1016/j.cemconres.2018.05.006>
6. Mechtcherine, V., et al.: Integrating reinforcement in digital fabrication with concrete: A review and classification framework. *Cement Concr. Compos.* **119**, 103964 (2021). <https://doi.org/10.1016/j.cemconcomp.2021.103964>

7. Lloret-Fritschi, E., et al.: From smart dynamic casting to a growing family of digital casting systems. *Cem. Concr. Res.* **134** (2020). <https://doi.org/10.1016/j.cemconres.2020.106071>
8. Kloft, H., Empelmann, M., Hack, N., Herrmann, E., Lowke, D.: Reinforcement strategies for 3D-concrete-printing. *Civil Eng. Design* **2**(4), 131–139 (2020). <https://doi.org/10.1002/cend.202000022>
9. Bos, F.P., Ahmed, Z.Y., Wolfs, R.J.M., Salet, T.A.M.: 3D printing concrete with reinforcement. In: Hordijk, D.A., Luković, M. (eds.) *High Tech Concrete: Where Technology and Engineering Meet*, pp. 2484–2493. Springer, Cham (2018). https://doi.org/10.1007/978-3-319-59471-2_283
10. Classen, M., Ungermann, J., Sharma, R.: Additive manufacturing of reinforced concrete—Development of a 3D printing technology for cementitious composites with metallic reinforcement. *Appl. Sci.* **10**(11), 3791 (2020). <https://doi.org/10.3390/app10113791>
11. Prüfverfahren für Zement - Teil 1: Bestimmung der Festigkeit: Deutsche Fassung EN 196-1:2016, DIN EN 196-1:2016-11, Deutsches Institut für Normung e.V., Berlin (2016)
12. Betonstahl - Teil 1: Stahlsorten, Eigenschaften, Kennzeichnung, DIN 488-1:2009-08, Deutsches Institut für Normung e.V. (DIN), Berlin (2009)
13. RILEM, Bond test for reinforcement steel: 2. Pull-out test (1983)
14. Bielak, J.: Shear in slabs with non-metallic reinforcement. Dissertation, Lehrstuhl und Institut für Massivbau. RWTH Aachen University, Aachen (2021)
15. Tragwerke aus Beton, Stahlbeton und Spannbeton – Teil 2: Beton – Festlegung, Eigenschaften, Herstellung und Konformität – Anwendungsregeln zu DIN EN 206-1, DIN 1045-2:2008-08, Deutsches Institut für Normung e.V. (DIN), Berlin (2008)